

Synthesis, Spectroscopic and Structural Studies on Six- and Eight-Coordinate Phosphane and Arsane Complexes of Titanium(IV) Halides

Richard Hart,^[a] William Levason,^[a] Bhavesh Patel,^[a] and Gillian Reid*^[a]

Keywords: Titanium / Halides / Phosphanes / Arsanes / Structure elucidation

The six-coordinate complexes $[\text{TiX}_4(\text{L-L})]$ [$\text{X} = \text{Cl}$ or Br ; $\text{L-L} = \text{Ph}_2\text{PCH}_2\text{PPh}_2$, $\text{Ph}_2\text{P}(\text{CH}_2)_2\text{PPh}_2$, $\text{Ph}_2\text{P}(\text{CH}_2)_3\text{PPh}_2$, $o\text{-C}_6\text{H}_4(\text{PPh}_2)_2$, $o\text{-C}_6\text{H}_4(\text{PMe}_2)_2$, $\text{Ph}_2\text{As}(\text{CH}_2)_2\text{AsPh}_2$, $o\text{-C}_6\text{H}_4(\text{AsMe}_2)_2$ or $\text{MeC}(\text{CH}_2\text{AsMe}_2)_3$] and the eight-coordinate complexes $[\text{TiX}_4(\text{L-L})_2]$ [$\text{L-L} = o\text{-C}_6\text{H}_4(\text{PMe}_2)_2$ or $o\text{-C}_6\text{H}_4(\text{AsMe}_2)_2$] have been prepared and characterised by solution ^1H and $^{31}\text{P}\{^1\text{H}\}$ NMR spectroscopy, IR and UV/Visible spectroscopy and microanalyses. The crystal structures of

$[\text{TiCl}_4\{o\text{-C}_6\text{H}_4(\text{PMe}_2)_2\}]$, $[\text{TiCl}_4\{o\text{-C}_6\text{H}_4(\text{PMe}_2)_2\}_2]$, $[\text{TiBr}_4\{o\text{-C}_6\text{H}_4(\text{PMe}_2)_2\}_2]$, $[\text{TiBr}_4\{o\text{-C}_6\text{H}_4(\text{AsMe}_2)_2\}_2]$ and $[\text{TiBr}_4\{\text{MeC}(\text{CH}_2\text{AsMe}_2)_3\}]$ are described and permit detailed comparisons to be made between the six- and eight-coordinate species and between the phosphane and arsane species. The crystal structure of the zwitterionic $[\text{TiCl}_5(\text{Ph}_2\text{PCH}_2\text{PPh}_2)]$ is also reported.

Introduction

Recently we have been investigating the chemistry of the early transition metal ions, particularly Ti^{IV} , with thio-, seleno- and telluroether ligands. Part of the impetus for this work arises from the potential of the resultant complexes as single-source precursors for transition metal chalcogenides through CVD processes. Thus, we have reported the preparation of a wide range of six-coordinate, distorted octahedral complexes of the form $[\text{TiX}_4(\text{E-E})]$ ($\text{E-E} = \text{dithio- or diselenoether}$).^[1] We have also isolated six- and seven-coordinate species involving trithio- and triselenoether ligands.^[2] In the course of this work we attempted to generate eight-coordinate species of the form $[\text{TiX}_4(\text{E-E})_2]$; however we saw no evidence at any stage for their existence either in solution or in the solid state. This prompted us to examine in some more detail the literature describing eight-coordinate Ti^{IV} complexes involving diphosphane and diarsane ligands. While a number of references to such species have been made, including, for example, $[\text{TiCl}_4\{o\text{-C}_6\text{H}_4(\text{PMe}_2)_2\}_2]$, $[\text{TiX}_4\{o\text{-C}_6\text{H}_4(\text{AsMe}_2)_2\}_2]$ ($\text{X} = \text{Cl}$ or Br) and $[\text{TiCl}_4\{\text{Me}_2\text{P}(\text{CH}_2)_2\text{PMe}_2\}_2]$,^[3–8] the literature is in fact very patchy and single crystal X-ray structural data are only available for two examples: an early report by Nyholm and co-workers on $[\text{TiCl}_4\{o\text{-C}_6\text{H}_4(\text{AsMe}_2)_2\}_2]$,^[3,4] and $[\text{TiCl}_4\{\text{Me}_2\text{P}(\text{CH}_2)_2\text{PMe}_2\}_2]$, which was reported by Cotton and co-workers in 1998.^[6] The synthesis of $[\text{TiCl}_4\{o\text{-C}_6\text{H}_4(\text{PMe}_2)_2\}_2]$ has been reported, but structural information is limited to an X-ray powder photograph, indicating the same structure as $[\text{TiCl}_4\{o\text{-C}_6\text{H}_4(\text{AsMe}_2)_2\}_2]$.^[5] This lack of structural data and the absence of any detailed solution studies on either the six- or eight-coordinate systems has prompted us to conduct more thorough studies on the synthesis and properties of phosphane and arsane com-

plexes of Ti^{IV} . Our specific aims were to investigate the possibility of forming other complexes with coordination numbers greater than six and to establish the structural consequences of changing from six- to eight-coordination. In this paper we report the results of our studies, including the preparations and spectroscopic characterisation of six- or eight-coordinate Ti^{IV} halide complexes involving $\text{Ph}_2\text{PCH}_2\text{PPh}_2$, $\text{Ph}_2\text{P}(\text{CH}_2)_2\text{PPh}_2$, $\text{Ph}_2\text{P}(\text{CH}_2)_3\text{PPh}_2$, $o\text{-C}_6\text{H}_4(\text{PPh}_2)_2$, $o\text{-C}_6\text{H}_4(\text{PMe}_2)_2$, $\text{Ph}_2\text{As}(\text{CH}_2)_2\text{AsPh}_2$, $o\text{-C}_6\text{H}_4(\text{AsMe}_2)_2$ and $\text{MeC}(\text{CH}_2\text{AsMe}_2)_3$. The crystal structures of $[\text{TiCl}_4\{o\text{-C}_6\text{H}_4(\text{PMe}_2)_2\}]$, $[\text{TiCl}_4\{o\text{-C}_6\text{H}_4(\text{PMe}_2)_2\}_2]$, $[\text{TiBr}_4\{o\text{-C}_6\text{H}_4(\text{PMe}_2)_2\}_2]$, $[\text{TiBr}_4\{o\text{-C}_6\text{H}_4(\text{AsMe}_2)_2\}_2]$ and $[\text{TiBr}_4\{\text{MeC}(\text{CH}_2\text{AsMe}_2)_3\}]$ are also described and permit the details of the structural changes incurred upon changing the Ti^{IV} coordination to be examined. The crystal structure of the unusual zwitterionic species $[\text{TiCl}_5(\text{PPh}_2\text{PCH}_2\text{PPh}_2)]$, which was obtained as a decomposition product from a solution of $[\text{TiCl}_4(\text{Ph}_2\text{PCH}_2\text{PPh}_2)]$, is also presented.

Results and Discussion

Compounds TiX_4 ($\text{X} = \text{Cl}$ or Br) react with one molar equivalent of L-L [$\text{L-L} = \text{Ph}_2\text{P}(\text{CH}_2)_n\text{PPh}_2$ ($n = 1-3$), $o\text{-C}_6\text{H}_4(\text{PMe}_2)_2$, $o\text{-C}_6\text{H}_4(\text{PPh}_2)_2$, $o\text{-C}_6\text{H}_4(\text{AsMe}_2)_2$ or $\text{Ph}_2\text{As}(\text{CH}_2)_2\text{AsPh}_2$] in rigorously anhydrous CH_2Cl_2 solution under an N_2 atmosphere to afford the 1:1 species $[\text{TiX}_4(\text{L-L})]$ as orange- or red-coloured solids in good yield; the tripodal ligand $\text{MeC}(\text{CH}_2\text{AsMe}_2)_3$ gives $[\text{TiX}_4\{\text{MeC}(\text{CH}_2\text{AsMe}_2)_3\}]$ also in high yield. The 1:2 complexes $[\text{TiX}_4\{o\text{-C}_6\text{H}_4(\text{PMe}_2)_2\}_2]$ and $[\text{TiX}_4\{o\text{-C}_6\text{H}_4(\text{AsMe}_2)_2\}_2]$ were obtained in good yield by similar reactions using two molar equivalents of ligand. The compounds are relatively stable as solids when stored under N_2 in a dry glove-box. However, in solution they are very susceptible to hydrolysis, rapidly decolourising. The powdered solids are also readily hydrolysed in moist air. For these

^[a] Department of Chemistry, University of Southampton, Highfield, Southampton SO17 1BJ, UK
Fax: (internat.) +44-23/8059-3781
E-mail: gr@soton.ac.uk

reasons all measurements were conducted using solutions freshly prepared in rigorously anhydrous solvents. IR spectra were recorded as nujol mulls and the complexes $[\text{TiX}_4(\text{L-L})]$ show, in addition to peaks due to the coordinated phosphane or arsane ligand, up to four bands around $420\text{--}350\text{ cm}^{-1}$ ($\text{X} = \text{Cl}$) or $320\text{--}280\text{ cm}^{-1}$ ($\text{X} = \text{Br}$), consistent with the presence of the *cis*-octahedral species (theory $2a_1 + b_1 + b_2$ for C_{2v} symmetry). Similar frequencies were observed for the tetrahalo-titanium thio- and selenoether species reported earlier.^[1] For the complexes $[\text{TiX}_4(\text{L-L})_2]$ [$\text{L-L} = o\text{-C}_6\text{H}_4(\text{PMe}_2)_2$ or $o\text{-C}_6\text{H}_4(\text{AsMe}_2)_2$], IR spectroscopy shows two peaks around 315 cm^{-1} for the chloro species and ca. 290 cm^{-1} for the bromo species (theory $b_2 + e$ for D_{2d} symmetry). The frequencies for the eight-coordinate species are generally significantly lower than for their six-coordinate analogues. These data are in good agreement with the literature.^[5]

Electronic spectra were recorded by diffuse reflectance owing to the highly sensitive nature of the compounds in solution. For the six-coordinate d^0 complexes $[\text{TiCl}_4(\text{L-L})]$, two broad features are present at ca. 21,000 and ca. 28,000 cm^{-1} , which may be assigned as $\sigma(\text{P,As}) \rightarrow \text{Ti}(t_{2g})$ and $\pi(\text{Cl}) \rightarrow \text{Ti}(t_{2g})$ LMCT transitions, respectively. Although the actual symmetry at Ti is C_{2v} , rather than O_h , the lifting of the degeneracy of the Ti t_{2g} orbitals does not result in resolved splittings, although it may contribute to the broadness of the bands. The spectra of the $[\text{TiBr}_4(\text{L-L})]$ complexes are less well resolved, but features at ca. 20,000 and 23,000 cm^{-1} are assigned similarly as $\sigma(\text{P,As}) \rightarrow \text{Ti}(t_{2g})$ and $\pi(\text{Br}) \rightarrow \text{Ti}(t_{2g})$ transitions. The $\sigma(\text{P,As}) \rightarrow \text{Ti}(t_{2g})$ transition appears at slightly lower energy when $\text{X} = \text{Br}$ than when $\text{X} = \text{Cl}$, an effect often observed with later transition metals.^[9] The eight-coordinate $[\text{TiX}_4(\text{L-L})_2]$ complexes have broad features at similar energies to their six-coordinate analogues, which are similarly assigned to LMCT transitions. For a D_{2d} metal centre, taking the *z*-axis as the principle inversion (S_4) axis, the lowest d-level is b_1 and thus the transitions are $\text{L} \text{ (or X)} \rightarrow \text{Ti}(b_1)$. A careful comparison of the diffuse reflectance spectra of the corresponding $[\text{TiCl}_4(\text{L-L})]$ and $[\text{TiCl}_4(\text{L-L})_2]$ complexes shows two differences: (i) the bands are broader in the eight-coordinate than in the six-coordinate complexes, and (ii) the $\sigma(\text{P,As}) \rightarrow \text{Ti}$ transitions are relatively more intense than the $\pi(\text{X}) \rightarrow \text{Ti}$ transition in the former, which is reasonable since the number of P/As donors has doubled. The bands in the spectra of $[\text{TiBr}_4(\text{L-L})_x]$ ($x = 1$ or 2) are very broad, but appear to show a similar trend. Whilst the six- and eight-coordinate complexes can be distinguished by their diffuse reflectance spectra when the spectra for both species are compared; the differences do not appear to be sufficiently large to assign the coordination number to a $\text{TiX}_4(\text{L-L})_x$ complex on the basis of the spectrum of only one or the other with any confidence.

Solution NMR studies

The $^{31}\text{P}\{^1\text{H}\}$ NMR spectrum of $[\text{TiCl}_4\{o\text{-C}_6\text{H}_4(\text{PMe}_2)_2\}_2]$ in CH_2Cl_2 at room temperature is a singlet

at $\delta = 31.5$, whereas that of the poorly soluble $[\text{TiCl}_4\{o\text{-C}_6\text{H}_4(\text{PMe}_2)_2\}]$ has $\delta = 29.5$. The corresponding ^1H NMR spectra show second order multiplets for the PMe_2 groups at $\delta = 1.88$ ($[\text{TiCl}_4\{o\text{-C}_6\text{H}_4(\text{PMe}_2)_2\}_2]$) and 1.90 ($[\text{TiCl}_4\{o\text{-C}_6\text{H}_4(\text{PMe}_2)_2\}]$) and the spectra are essentially unchanged on cooling the solution to -90°C . We therefore conclude that neither complex dissociates ligand under these conditions. Similar studies on $[\text{TiBr}_4\{o\text{-C}_6\text{H}_4(\text{PMe}_2)_2\}]$ reveal a single $^{31}\text{P}\{^1\text{H}\}$ NMR resonance at $\delta = 24.5$, and addition of $o\text{-C}_6\text{H}_4(\text{PMe}_2)_2$ to this solution produces, in addition to a free ligand resonance at $\delta = -55$, a new species at $\delta = 22.2$. The $^{31}\text{P}\{^1\text{H}\}$ NMR spectrum of $[\text{TiBr}_4\{o\text{-C}_6\text{H}_4(\text{PMe}_2)_2\}_2]$ at ambient temperatures contains three resonances at $\delta = 24.5$, 22.2 and -54 , from which it is clear that $[\text{TiBr}_4\{o\text{-C}_6\text{H}_4(\text{PMe}_2)_2\}_2]$ is partially dissociated in solution into the 1:1 complex and $o\text{-C}_6\text{H}_4(\text{PMe}_2)_2$, and that exchange between either complex and $o\text{-C}_6\text{H}_4(\text{PMe}_2)_2$ is slow on the ^{31}P NMR time-scale at ambient temperatures. The ^1H NMR spectra lead to similar conclusions, although the coordinated PMe_2 resonances overlap. The $^{31}\text{P}\{^1\text{H}\}$ NMR spectrum of $[\text{TiCl}_4\{o\text{-C}_6\text{H}_4(\text{PPh}_2)_2\}]$ shows a sharp singlet at $\delta = 34.2$, and that of $[\text{TiCl}_4\{\text{Ph}_2\text{P}(\text{CH}_2)_2\text{PPh}_2\}]$ a singlet at $\delta = 24.6$. The spectra of the corresponding bromides and of $[\text{TiX}_4\{\text{Ph}_2\text{P}(\text{CH}_2)_3\text{PPh}_2\}]$ show only very broad resonances at lower frequency which remain broad even at -90°C ; we attribute this to reversible ligand dissociation.

For the $o\text{-C}_6\text{H}_4(\text{AsMe}_2)_2$ complexes only ^1H NMR spectroscopic data were available (attempts to study ligand exchange in solution by $^{13}\text{C}\{^1\text{H}\}$ NMR were unsuccessful due mainly to poor solubility). At room temperature the complex $[\text{TiCl}_4\{o\text{-C}_6\text{H}_4(\text{AsMe}_2)_2\}]$ showed a singlet AsMe_2 resonance at $\delta = 1.75$, whereas $[\text{TiCl}_4\{o\text{-C}_6\text{H}_4(\text{AsMe}_2)_2\}_2]$ contained three resonances at $\delta = 1.8$, 1.74 and 1.2 . The $\delta = 1.2$ resonance is due to free $o\text{-C}_6\text{H}_4(\text{AsMe}_2)_2$, and thus the spectrum shows that $[\text{TiCl}_4\{o\text{-C}_6\text{H}_4(\text{AsMe}_2)_2\}_2]$ is partially dissociated into the 1:1 complex and $o\text{-C}_6\text{H}_4(\text{AsMe}_2)_2$. Attempts to record spectra at -90°C were unsuccessful due to the poor solubility of the complex at low temperatures. The spectrum obtained from $[\text{TiBr}_4\{o\text{-C}_6\text{H}_4(\text{AsMe}_2)_2\}]$ in CD_2Cl_2 at room temperature shows an AsMe_2 singlet at $\delta = 1.9$ (assigned to the complex) and some free $o\text{-C}_6\text{H}_4(\text{AsMe}_2)_2$ at $\delta = 1.2$. The spectrum of $[\text{TiBr}_4\{o\text{-C}_6\text{H}_4(\text{AsMe}_2)_2\}_2]$ contained broad lines at $\delta = 1.9$ and 1.2 attributable to the 1:1 complex and free ligand; a weaker peak at $\delta = 1.6$ is tentatively attributed to the 2:1 complex. These resonances sharpened on cooling.

Comparison of these results show that whilst the $[\text{TiCl}_4\{o\text{-C}_6\text{H}_4(\text{PMe}_2)_2\}_n]$ ($n = 1$ or 2) and $[\text{TiBr}_4\{o\text{-C}_6\text{H}_4(\text{PMe}_2)_2\}]$ complexes are stable in solution, the $[\text{TiCl}_4\{o\text{-C}_6\text{H}_4(\text{AsMe}_2)_2\}_2]$ and $[\text{TiBr}_4\{o\text{-C}_6\text{H}_4(\text{PMe}_2)_2\}_2]$ complexes are partially dissociated in solution into the corresponding 1:1 complex and free ligand. Greater dissociation is observed with the weaker Lewis acid TiBr_4 : $[\text{TiBr}_4\{o\text{-C}_6\text{H}_4(\text{AsMe}_2)_2\}]$ appears to be partially dissociated into TiBr_4 and $o\text{-C}_6\text{H}_4(\text{AsMe}_2)_2$ in solution. Of the complexes of the phenyl-substituted diphosphanes, only the $[\text{TiCl}_4(\text{L-L})]$ [$\text{L-L} = \text{Ph}_2\text{P}(\text{CH}_2)_2\text{PPh}_2$ or $o\text{-C}_6\text{H}_4(\text{PPh}_2)_2$] show sharp ^{31}P NMR spectra; in the corresponding brom-

ides or in $[\text{TiCl}_4\{\text{Ph}_2\text{P}(\text{CH}_2)_3\text{PPh}_2\}]$, only very broad lines, typical of rapidly exchanging systems are observed.

The $[\text{TiX}_4\{\text{MeC}(\text{CH}_2\text{AsMe}_2)_3\}]$ systems were difficult to study in solution due to their very poor solubility in chlorocarbons, and attempts to obtain $^{13}\text{C}\{^1\text{H}\}$ data were unsuccessful. However, the ^1H NMR spectroscopic data are consistent with the six-coordinate structure established crystallographically for the bromide. Both show an uncoordinated AsMe_2 resonance at $\delta = 0.95$, coordinated AsMe_2 groups (broad singlet at $\delta = 1.71$ for $\text{X} = \text{Br}$, and two lines of 1:1 intensity $\delta = 1.59, 1.61$ $\text{X} = \text{Cl}$) and corresponding CH_2 resonances near $\delta = 2.0$ (coord) and $\delta = 1.7$ (free). The spectra show that exchange between the free and coordinated arms of the tridentate arsane is slow at ambient temperatures, which contrasts with the behaviour in the trithioether analogues.^[2] These conclusions are at odds with an early literature report^[10] which concludes from ^1H NMR spectroscopy that $[\text{TiCl}_4\{\text{MeC}(\text{CH}_2\text{AsMe}_2)_3\}]$ is seven-coordinate with tridentate triarsane coordination. This was subsequently questioned by McAlees and co-workers^[11] who reinterpreted the original NMR spectroscopic data and suggested six-coordination, with one arm of the tripod uncoordinated. Our conclusions are also supported by a single crystal X-ray structure determination (see below).

X-ray Crystallographic Studies

Crystals of $[\text{TiCl}_4\{o\text{-C}_6\text{H}_4(\text{PMe}_2)_2\}]$, $[\text{TiCl}_4\{o\text{-C}_6\text{H}_4(\text{PMe}_2)_2\}_2]$, $[\text{TiBr}_4\{o\text{-C}_6\text{H}_4(\text{PMe}_2)_2\}_2]$, $[\text{TiBr}_4\{o\text{-C}_6\text{H}_4(\text{AsMe}_2)_2\}_2]$ and $[\text{TiBr}_4\{\text{MeC}(\text{CH}_2\text{AsMe}_2)_3\}]$ were obtained from CH_2Cl_2 solution. The structure of $[\text{TiCl}_4\{o\text{-C}_6\text{H}_4(\text{PMe}_2)_2\}]$ (Figure 1) shows a discrete distorted octahedral geometry at Ti^{IV} , with the $o\text{-C}_6\text{H}_4(\text{PMe}_2)_2$ ligand chelating. The Ti–P bond lengths of 2.5733(13) and 2.5600(12) Å are in agreement with those in $[\text{TiCl}_4\{\text{Me}_2\text{P}(\text{CH}_2)_2\text{PMe}_2\}]$ [2.574(2) – 2.590(2) Å] and other six-coordinate phosphane complexes of Ti^{IV} .^[12,13] The Ti–Cl distances *trans* to Cl are longer than those *trans* to P by ca. 0.2 Å, consistent with a *trans* influence on Ti^{IV} of $\text{Cl} > \text{P}$. A similar trend was observed for $[\text{TiX}_4(\text{E}-\text{E})]$ (E–E = dithioether or diselenoether), where the *trans* influence was $\text{X} > \text{E}$, and $[\text{TiCl}_4\{\text{Me}_2\text{P}(\text{CH}_2)_2\text{PMe}_2\}]$ and $[\text{TiCl}_4\{\text{Et}_2\text{P}(\text{CH}_2)_2\text{PETe}_2\}]$.^[12,13] The axial $\text{Cl}(3)\text{--Ti}(1)\text{--Cl}(4)$ unit is tilted to lie over the $o\text{-C}_6\text{H}_4(\text{PMe}_2)_2$ ligand, with an angle of 164.25(6)°. The P–Ti–P angle in the five-membered chelate ring is constrained to be 76.05(4)°.

Crystals were also obtained for the directly comparable eight-coordinate species $[\text{TiCl}_4\{o\text{-C}_6\text{H}_4(\text{PMe}_2)_2\}_2]$, although the crystal quality was less good, resulting in higher residuals. However, the structure of this complex (Figure 2) shows crystallographic 4 $\bar{2}$ symmetry and adopts a dodecahedral stereochemistry. The Ti–Cl distance [2.503(3) Å] is 0.20–0.25 Å longer than in the six-coordinate $[\text{TiCl}_4\{o\text{-C}_6\text{H}_4(\text{PMe}_2)_2\}]$. This is substantially greater than the increase in $d(\text{Ti}^{\text{IV}}\text{--P})$ which is ca. 0.1 Å on going from a six- to an eight-coordinate geometry. Normally one would expect an increase in coordination number to be accompanied by an increase in Ti–donor atom bond length. Indeed,

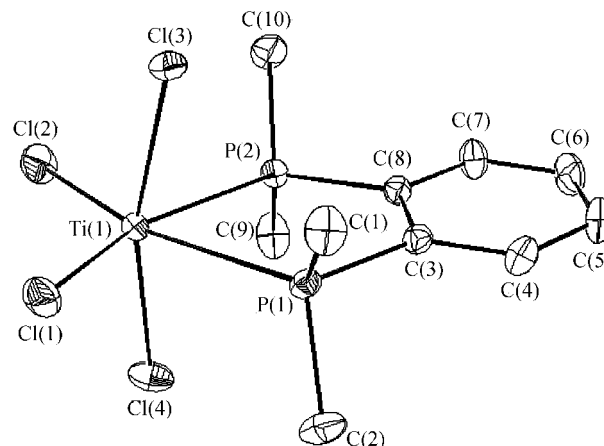


Figure 1. View of the structure of $[\text{TiCl}_4\{o\text{-C}_6\text{H}_4(\text{PMe}_2)_2\}]$ with atom numbering scheme; ellipsoids are shown at the 40% probability level; selected bond lengths (Å) and angles (°): Ti(1)–Cl(1) 2.2748(12), Ti(1)–Cl(2) 2.253(1), Ti(1)–Cl(3) 2.2975(13), Ti(1)–Cl(4) 2.2938(13); Ti(1)–P(1) 2.5733(13), Ti(1)–P(2) 2.5600(12); Cl(1)–Ti(1)–Cl(2) 114.58(5), Cl(1)–Ti(1)–Cl(3) 93.88(5), Cl(1)–Ti(1)–Cl(4) 94.23(5), Cl(1)–Ti(1)–P(1) 84.39(5), Cl(1)–Ti(1)–P(2) 160.39(5), Cl(2)–Ti(1)–Cl(3) 94.42(5), Cl(2)–Ti(1)–Cl(4) 94.44(5), Cl(2)–Ti(1)–P(1) 161.00(5), Cl(2)–Ti(1)–P(2) 84.96(5), Cl(3)–Ti(1)–Cl(4) 164.25(6), Cl(3)–Ti(1)–P(1) 82.80(4), Cl(3)–Ti(1)–P(2) 82.39(4), Cl(4)–Ti(1)–P(1) 84.59(5), Cl(4)–Ti(1)–P(2) 85.45(5), P(1)–Ti(1)–P(2) 76.05(4).

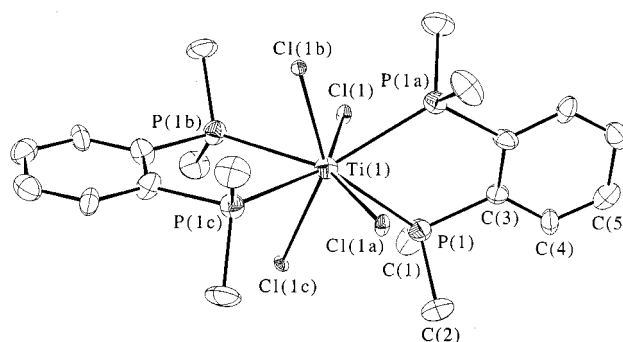


Figure 2. View of the structure of $[\text{TiCl}_4\{o\text{-C}_6\text{H}_4(\text{PMe}_2)_2\}_2]$ with atom numbering scheme; ellipsoids are shown at the 40% probability level; symmetry operators $-x, -y, z; 1/2 - y, 1/2 + x, 1/2 - z; 1/2 + y, 1/2 - x, 1/2 - z$; selected bond lengths (Å) and angles (°): Ti(1)–Cl(1) 2.503(3), Ti(1)–P(1) 2.654(4); Cl(1)–Ti(1)–Cl(1b) 95.23(3), Cl(1)–Ti(1)–Cl(1a) 144.85(11), Cl(1)–Ti(1)–P(1) 75.97(12), Cl(1)–Ti(1)–P(1a) 75.88(12), Cl(1)–Ti(1)–P(1b) 71.22(10), Cl(1)–Ti(1)–P(1c) 143.93(10).

this is clearly true for these systems, although the increase in bond length is different for Ti–P than for Ti–Cl. In the six-coordinate species the high *trans* influence of Cl on Ti^{IV} lengthens the Ti–P bond and indeed shortens the Ti–Cl *trans* P bond length (above). In the eight-coordinate flattened dodecahedron, however, the P–Ti–Cl angles are all less than 145°, and this will reduce the magnitude of the *trans* influence of the Cl ligands, thus accounting for some of the disparity. The P–Ti–P angle in the chelate ring is reduced to 72.7(2)° upon increasing the coordination number, a direct consequence of the longer Ti–P bond lengths.

The same geometry has been identified for $[\text{TiCl}_4\{\text{Me}_2\text{P}(\text{CH}_2)_2\text{PMe}_2\}_2]$, although in this case there is twofold crystallographic symmetry [$d(\text{Ti}-\text{P}) = 2.648(1)$, $2.654(1)$ Å; $d(\text{Ti}-\text{Cl}) = 2.446(1)$, $2.451(1)$ Å].^[6] $[\text{TiCl}_4\{o\text{-C}_6\text{H}_4(\text{AsMe}_2)_2\}_2]$ ^[3,4] is probably isostructural with the $[\text{TiCl}_4\{o\text{-C}_6\text{H}_4(\text{PMe}_2)_2\}_2]$ complex reported here, although few details of the crystallographic information are presented in the early reports [$d(\text{Ti}-\text{As}) = 2.71(2)$ Å; $d(\text{Ti}-\text{Cl}) = 2.46(2)$ Å].

The only other case where both the six- and eight-coordinate Ti^{IV} complexes of a single phosphane or arsane ligand have been structurally characterised involves $\text{Me}_2\text{P}(\text{CH}_2)_2\text{PMe}_2$. The structures of $[\text{TiCl}_4\{\text{Me}_2\text{P}(\text{CH}_2)_2\text{PMe}_2\}]$ and $[\text{TiCl}_4\{\text{Me}_2\text{P}(\text{CH}_2)_2\text{PMe}_2\}_2]$ were both reported by Cotton and co-workers,^[6,12] although in the former the phosphane ligand is disordered, making direct comparison of the structural details more difficult.

The crystals of $[\text{TiBr}_4\{o\text{-C}_6\text{H}_4(\text{PMe}_2)_2\}_2]$ (Figure 3) and $[\text{TiBr}_4\{o\text{-C}_6\text{H}_4(\text{AsMe}_2)_2\}_2]$ (Figure 4) are isostructural with $[\text{TiCl}_4\{o\text{-C}_6\text{H}_4(\text{PMe}_2)_2\}_2]$ above, although the crystal qual-

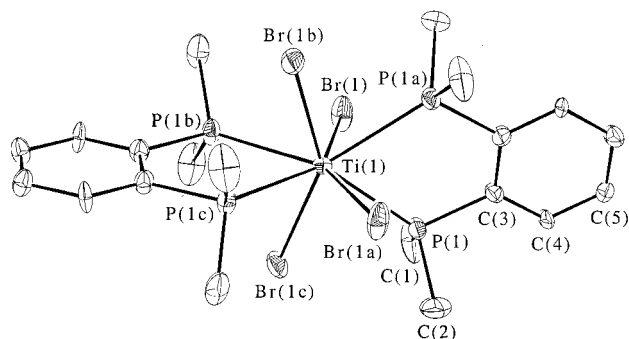


Figure 3. View of the structure of $[\text{TiBr}_4\{o\text{-C}_6\text{H}_4(\text{PMe}_2)_2\}_2]$ with atom numbering scheme; ellipsoids are shown at the 40% probability level; symmetry operators $-x, -y, z; y, -x, -z; -y, x, -z$; selected bond lengths (Å) and angles ($^\circ$): $\text{Ti}(1)-\text{Br}(1)$ 2.5776(9), $\text{Ti}(1)-\text{P}(1)$ 2.672(2); $\text{Br}(1)-\text{Ti}(1)-\text{Br}(1a)$ 144.70(4), $\text{Br}(1)-\text{Ti}(1)-\text{Br}(1b)$ 95.276(13), $\text{Br}(1)-\text{Ti}(1)-\text{P}(1)$ 75.89(7), $\text{Br}(1)-\text{Ti}(1)-\text{P}(1a)$ 75.86(7), $\text{Br}(1)-\text{Ti}(1)-\text{P}(1b)$ 71.22(6), $\text{Br}(1)-\text{Ti}(1)-\text{P}(1c)$ 144.08(5).

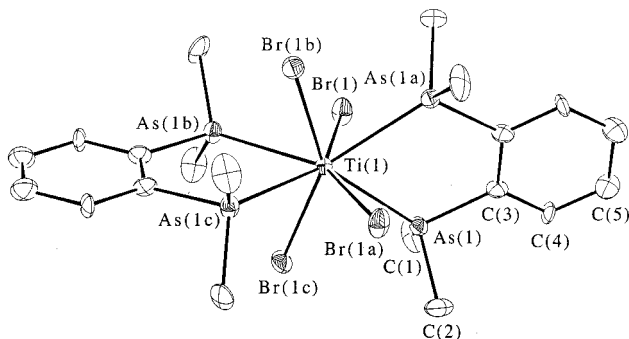


Figure 4. View of the structure of $[\text{TiBr}_4\{o\text{-C}_6\text{H}_4(\text{AsMe}_2)_2\}_2]$ with atom numbering scheme; ellipsoids are shown at the 40% probability level; symmetry operators $-x, -y, z; y, -x, -z; -y, x, -z$; selected bond lengths (Å) and angles ($^\circ$): $\text{Ti}(1)-\text{Br}(1)$ 2.5869(12), $\text{Ti}(1)-\text{As}(1)$ 2.7324(13); $\text{Br}(1)-\text{Ti}(1)-\text{Br}(1a)$ 144.77(6), $\text{Br}(1)-\text{Ti}(1)-\text{Br}(1b)$ 95.26(2), $\text{Br}(1)-\text{Ti}(1)-\text{As}(1)$ 75.98(5), $\text{Br}(1)-\text{Ti}(1)-\text{As}(1a)$ 75.92(5), $\text{Br}(1)-\text{Ti}(1)-\text{As}(1b)$ 70.94(4), $\text{Br}(1)-\text{Ti}(1)-\text{As}(1c)$ 144.29(4).

ity was significantly better in these, leading to better structure definition and lower esd's on the geometric parameters. The $\text{Ti}-\text{Br}$ and $\text{Ti}-\text{P}$ distances in $[\text{TiBr}_4\{o\text{-C}_6\text{H}_4(\text{PMe}_2)_2\}_2]$ are 2.5776(9), 2.672(2) Å, respectively. The latter is in agreement with the $\text{Ti}-\text{P}$ distance in $[\text{TiCl}_4\{o\text{-C}_6\text{H}_4(\text{PMe}_2)_2\}_2]$. The $\text{Ti}-\text{As}$ distance in $[\text{TiBr}_4\{o\text{-C}_6\text{H}_4(\text{AsMe}_2)_2\}_2]$ is 2.7324(13) Å, similar to the value of 2.71(2) Å reported for $[\text{TiCl}_4\{o\text{-C}_6\text{H}_4(\text{AsMe}_2)_2\}_2]$.^[3,4] A comparison of the $\text{Ti}-\text{P}$ and $\text{Ti}-\text{As}$ distances in $[\text{TiBr}_4\{o\text{-C}_6\text{H}_4(\text{PMe}_2)_2\}_2]$ and $[\text{TiBr}_4\{o\text{-C}_6\text{H}_4(\text{AsMe}_2)_2\}_2]$ shows an increase of 0.06 Å upon changing from phosphane to arsane. This is slightly less than the differences observed for some other transition metal complexes of $o\text{-C}_6\text{H}_4(\text{PMe}_2)_2$ and $o\text{-C}_6\text{H}_4(\text{AsMe}_2)_2$. For example, $[\text{NiCl}_2\{o\text{-C}_6\text{H}_4(\text{PMe}_2)_2\}_2]^+$ has a $\text{Ni}-\text{P}$ bond length of 2.255(3) Å and $[\text{NiCl}_2\{o\text{-C}_6\text{H}_4(\text{AsMe}_2)_2\}_2]^+$ $\text{Ni}-\text{As}$ bond lengths of 2.339(3), 2.345(3) Å,^[14,15] while $[\text{CoCl}_2\{o\text{-C}_6\text{H}_4(\text{PMe}_2)_2\}_2]^+$ has an average $\text{Co}-\text{P}$ bond length of 2.261 Å and $[\text{CoCl}_2\{o\text{-C}_6\text{H}_4(\text{AsMe}_2)_2\}_2]^+$ an average $\text{Co}-\text{As}$ bond length of 2.334 Å.^[15,16]

The Ti^{IV} tetrahalo complexes of the tripodal $\text{MeC}(\text{CH}_2)_3\text{AsMe}_2$ were prepared in an attempt to obtain seven-coordinate species. NMR studies (above and ref.^[11]) indicate that these species in fact adopt six-coordinate geometries in solution with one arm of the $\text{MeC}(\text{CH}_2)_3\text{AsMe}_2$ ligand remaining uncoordinated. A crystal structure determination was also undertaken on $[\text{TiBr}_4\{\text{MeC}(\text{CH}_2)_3\text{AsMe}_2\}_2]$ to establish the solid state structure. This shows that the complex adopts a distorted octahedral coordination environment at Ti^{IV} , derived from four Br ligands and two mutually *cis* As atoms from the bidentate tripodal $\text{MeC}(\text{CH}_2)_3\text{AsMe}_2$ ligand (Figure 5). The remaining As atom is uncoordinated. Hence the structures adopted in solution and in the solid state are the same. The $\text{Ti}-\text{Br}$ distances in this species exhibit similar trends to the $\text{Ti}-\text{Cl}$ distances in the six-coordinate $[\text{TiCl}_4\{o\text{-C}_6\text{H}_4(\text{PMe}_2)_2\}_2]$ complex above, with the $\text{Ti}-\text{Br}(\text{trans}-\text{Br})$ distances significantly longer than those *trans* to the *trans* As atom. Also, the $\text{Ti}-\text{Br}$ distances in this six-coordinate species are significantly shorter than in the eight-coordinate $[\text{TiBr}_4\{o\text{-C}_6\text{H}_4(\text{PMe}_2)_2\}_2]$ complex above, while the $\text{Ti}-\text{As}$ distances [2.680(3), 2.686(2) Å] are ca. 0.05 Å shorter than in $[\text{TiBr}_4\{o\text{-C}_6\text{H}_4(\text{AsMe}_2)_2\}_2]$. These observations parallel the differences described above for the six- and eight-coordinate $\text{TiCl}_4/o\text{-C}_6\text{H}_4(\text{PMe}_2)_2$ systems.

A small number of crystals of $[\text{TiCl}_5(\text{Ph}_2\text{PCH}_2\text{PPh}_2)]$ were produced by partial decomposition of $[\text{TiCl}_4(\text{Ph}_2\text{PCH}_2\text{PPh}_2)]$ in CH_2Cl_2 solution, probably by hydrolysis and subsequent HCl addition. Although there was insufficient sample to permit full spectroscopic characterisation ($\nu_{\text{Ti}-\text{Cl}} = 360$ sh, 356, 344 sh), a crystal structure was obtained. The structure shows the phosphane ligand to be coordinated to a TiCl_5 fragment through a single phosphorus atom (Figure 6). A proton on the other P atom (giving a phosphonium function) was located in the difference map and is also inferred to achieve charge balance. Thus this species is an unusual zwitterionic complex with a distorted octahedral Ti^{IV} coordination geometry. The $\text{Ti}-\text{P}$

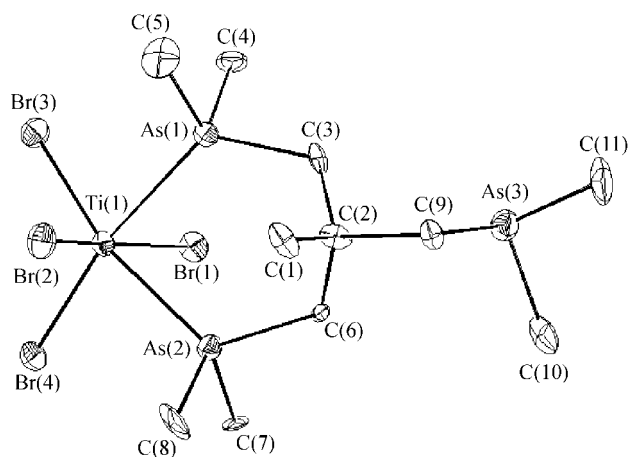


Figure 5. View of the structure of $[\text{TiBr}_4\{\text{MeC}(\text{CH}_2\text{AsMe}_2)_3\}]$ with atom numbering scheme; ellipsoids are shown at the 40% probability level; selected bond lengths (Å) and angles ($^\circ$): Br(1)–Ti(1) 2.471(3), Br(2)–Ti(1) 2.445(3), Br(3)–Ti(1) 2.407(3), Br(4)–Ti(1) 2.403(3), As(1)–Ti(1) 2.680(3), As(2)–Ti(1) 2.688(3); Br(1)–Ti(1)–Br(2) 162.3(1), Br(1)–Ti(1)–Br(3) 95.93(11), Br(1)–Ti(1)–Br(4) 95.97(11), Br(1)–Ti(1)–As(1) 82.57(10), Br(1)–Ti(1)–As(2) 81.53(10), Br(2)–Ti(1)–Br(3) 94.84(12), Br(2)–Ti(1)–Br(4) 93.93(11), Br(2)–Ti(1)–As(1) 84.78(10), Br(2)–Ti(1)–As(2) 84.70(10), Br(3)–Ti(1)–As(1) 83.36(10), Br(3)–Ti(1)–As(2) 166.30(13), Br(4)–Ti(1)–As(1) 168.4(1), Br(4)–Ti(1)–As(2) 85.39(10), As(1)–Ti(1)–As(2) 82.97(9)

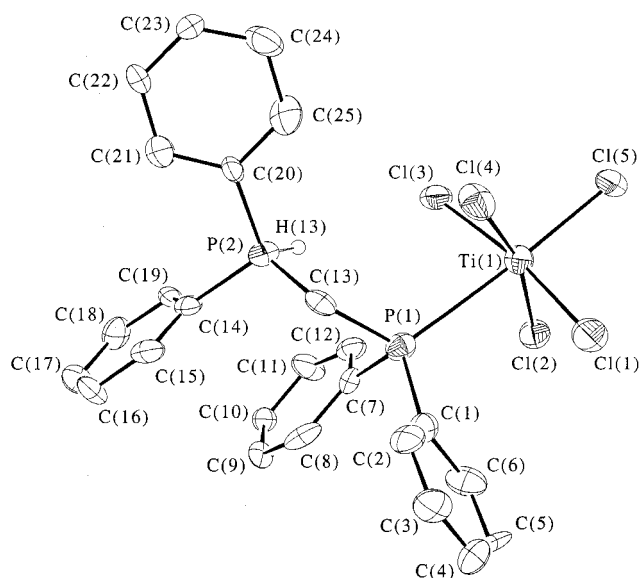


Figure 6. View of the structure of $[\text{TiCl}_5(\text{Ph}_2\text{PCH}_2\text{PPh}_2)]$ with atom numbering scheme; ellipsoids are shown at the 40% probability level; selected bond lengths (Å) and angles ($^\circ$): Ti(1)–Cl(1) 2.276(3), Ti(1)–Cl(2) 2.283(3), Ti(1)–Cl(3) 2.320(3), Ti(1)–Cl(4) 2.333(3), Ti(1)–Cl(5) 2.291(3), Ti(1)–P(1) 2.732(4), Cl(1)–Ti(1)–Cl(2) 95.67(12), Cl(1)–Ti(1)–Cl(3) 96.82(12), Cl(1)–Ti(1)–Cl(4) 93.02(13), Cl(1)–Ti(1)–Cl(5) 98.94(12), Cl(1)–Ti(1)–P(1) 176.52(13), Cl(2)–Ti(1)–Cl(3) 87.87(13), Cl(2)–Ti(1)–Cl(4) 171.2(1), Cl(2)–Ti(1)–Cl(5) 89.1(1), Cl(2)–Ti(1)–P(1) 87.62(12), Cl(3)–Ti(1)–Cl(4) 89.70(12), Cl(3)–Ti(1)–Cl(5) 164.18(13), Cl(3)–Ti(1)–P(1) 82.15(11), Cl(4)–Ti(1)–Cl(5) 90.92(12), Cl(4)–Ti(1)–P(1) 83.66(11), Cl(5)–Ti(1)–P(1) 82.20(10), P(1)–C(13)–P(2) 113.7(5)

distance in this species [2.732(4) Å] is considerably longer (by about 0.2 Å) than $d(\text{Ti}–\text{P})$ *trans* X in other six-coordinate complexes such as $[\text{TiCl}_4\{o\text{-C}_6\text{H}_4(\text{PMe}_2)_2\}]$, above, and $[\text{TiCl}_4\{\text{Me}_2\text{P}(\text{CH}_2)_2\text{PMe}_2\}]$.^[12] This substantial lengthening of $d(\text{Ti}–\text{P})$ in the zwitterionic complex may arise from deactivation of the P-based lone pair on the phosphane function upon quaternization of the adjacent P centre, leading to a weaker Ti–P interaction. Notably, the Ti–Cl distance *trans* to P is not very different to the other Ti–Cl distances, unlike the examples above, $[\text{TiCl}_4\{o\text{-C}_6\text{H}_4(\text{PMe}_2)_2\}]$ and $[\text{TiBr}_4\{\text{MeC}(\text{CH}_2\text{AsMe}_2)_3\}]$, where $d(\text{Ti}–\text{X})$ *trans* P/As is significantly shorter than $d(\text{Ti}–\text{X})$ *trans* X. The angles at Ti indicate a distorted octahedral geometry, but with the Cl(1)–Ti(1)–Cl angles all greater than 90° and, correspondingly, the P(1)–Ti(1)–Cl(*x*) (*x* = 2–5) angles all less than 90° . The consequence of this is that the Cl atoms in the TiCl_4 plane are displaced towards the phosphane ligand.

Conclusions

These results show that both six- and eight-coordinate Ti^{IV} complexes of $o\text{-C}_6\text{H}_4(\text{PMe}_2)_2$ and $o\text{-C}_6\text{H}_4(\text{AsMe}_2)_2$ may be isolated. Solution NMR studies show that the six-coordinate phosphane and arsane species do not undergo fast ligand exchange. On the other hand, the eight-coordinate complexes generally dissociate a ligand and exist in solution as an equilibrium mixture of $[\text{TiX}_4(\text{L-L})_2]$, $[\text{TiX}_4(\text{L-L})]$, TiX_4 and L-L. Attempts to prepare seven-coordinate Ti^{IV} complexes with $\text{MeC}(\text{CH}_2\text{AsMe}_2)_3$ yielded only the six-coordinate species, with the tripodal ligand functioning as a bidentate chelate. The six- and eight-coordinate complexes $[\text{TiCl}_4\{o\text{-C}_6\text{H}_4(\text{PMe}_2)_2\}]$ and $[\text{TiCl}_4\{o\text{-C}_6\text{H}_4(\text{PMe}_2)_2\}_2]$ have been crystallographically characterised and the structural consequences of converting from six- to eight-coordinate Ti^{IV} have been established.

Experimental Section

Infrared spectra were measured as Nujol mulls between CsI plates using a Perkin–Elmer 1710 spectrometer over the range 220–4000 cm^{-1} . ^1H NMR spectra were recorded in CDCl_3 or CD_2Cl_2 using a Bruker AM300 or DPX400 spectrometer. $^{13}\text{C}\{^1\text{H}\}$ and $^{31}\text{P}\{^1\text{H}\}$ NMR spectra were recorded at 300 K unless otherwise stated, using a Bruker DPX400 spectrometer operating at 100.6 and 162.0 MHz, respectively, and are referenced to TMS or external 85% H_3PO_4 . UV/Visible spectra were recorded by diffuse reflectance using a Perkin–Elmer Lambda19 spectrometer. Samples were diluted with BaSO_4 . Titanium halides were obtained from Aldrich and used as received. The ligands $o\text{-C}_6\text{H}_4(\text{PMe}_2)_2$, $o\text{-C}_6\text{H}_4(\text{PPh}_2)_2$, $\text{Ph}_2\text{As}(\text{CH}_2)_2\text{AsPh}_2$, $o\text{-C}_6\text{H}_4(\text{AsMe}_2)_2$ and $\text{MeC}(\text{CH}_2\text{AsMe}_2)_3$ were prepared by literature methods,^[17–20] while the other phosphane ligands were obtained from Aldrich. Dichloromethane and chloroform were dried by distillation from CaH_2 and hexane was dried by distillation from the sodium ketyl of benzophenone. Deuterated solvents were dried over molecular sieves. All preparations used rigorously anhydrous solvents and inert atmosphere techniques.

(i) **[TiCl₄(Ph₂PCH₂PPh₂)]:** Ph₂PCH₂PPh₂ (0.35 g, 0.91 mmol) was dissolved in dry, degassed hexane (20 cm³) in a Schlenk flask under an atmosphere of dry N₂. TiCl₄ (0.1 cm³, 0.91 mmol) was added with a syringe, resulting in immediate precipitation of a bright orange solid. The solution was stirred for ca. 30 min. and the solid filtered and dried in vacuo. Yield 0.45 g, 88%. C₂₅H₂₂Cl₄P₂Ti (574.11): calcd. C 52.3, H 3.8; found C 52.0, H 3.7. – IR: ν_{Ti–Cl} = 419, 398, 385, 375 cm^{–1}. – UV/Vis (λ_{max} × 10³ cm^{–1}): 20.7, 28.5sh, 34.8. – ¹H NMR (CDCl₃, 300 K): δ = 7.0–8.0 (m, Ph), 4.0 (t, ²J_{H–P} = 10 Hz, CH₂).

(ii) **[TiCl₄(Ph₂P(CH₂)₂PPh₂)]:** Method as for (i) above, orange solid, yield 0.43 g, 80%. C₂₆H₂₄Cl₄P₂Ti (588.14): calcd. C 53.0, H 4.1; found C 53.7, H 4.4. – IR: ν_{Ti–Cl} = 420, 398, 385, 376 cm^{–1}. – UV/Vis (λ_{max} × 10³ cm^{–1}): 20.7, 26.1sh, 34.8. – ¹H NMR (CDCl₃, 300 K): δ = 7.1–7.9 (m, Ph), 3.0 (d, CH₂, ²J_{H–P} = 13 Hz). – ³¹P{¹H} NMR (CH₂Cl₂/CD₂Cl₂): δ = 24.6.

(iii) **[TiCl₄{Ph₂P(CH₂)₃PPh₂}]:** Method as for (i) above, orange solid, yield 0.49 g, 91%. C₂₇H₂₆Cl₄P₂Ti (602.16): calcd. C 53.8, H 4.3; found C 53.6, H 4.4. – IR: ν_{Ti–Cl} = 417, 394, 369 cm^{–1}. – UV/Vis (λ_{max} × 10³ cm^{–1}): 20.7, 27.8 sh, 37.7. – ¹H NMR (CDCl₃, 300 K): δ = 7.2–7.8 (m, Ph), 2.7 (t, CH₂), 2.2 (q, CH₂). – ³¹P{¹H} NMR (CH₂Cl₂): 2.3 (very broad).

(iv) **[TiCl₄{*o*-C₆H₄(PPh₂)₂}]:** Method as for (i) above, orange solid, yield 0.69 g, 81%. C₃₀H₂₄Cl₄P₂Ti: calcd. C 56.6, H 3.8; found C 56.3, H 3.9. – IR: ν_{Ti–Cl} = 420, 408, 386, 375 cm^{–1}. – UV/Vis (λ_{max} × 10³ cm^{–1}): 21.3, 26.0sh, 32.3. – ¹H NMR (CDCl₃, 300 K): δ = 7.0–8.2 (m, Ph). – ³¹P{¹H} NMR (CH₂Cl₂/CDCl₃): δ = 34.1.

(v) **[TiCl₄{*o*-C₆H₄(PMe₂)₂}]:** Method as for (i) above, pale yellow solid, yield 0.10 g, 57%. C₁₀H₁₆Cl₄P₂Ti (387.90): calcd. C 31.0, H 4.2; found C 31.2, H 4.3. – IR: ν_{Ti–Cl} = 420, 410, 382 cm^{–1}. – UV/Vis (λ_{max} × 10³ cm^{–1}): 22.7, 28.6, 33.0. – ¹H NMR (CDCl₃, 300 K): δ = 7.6 (m, *o*-C₆H₄), 1.9 (m, Me). – ³¹P{¹H} NMR (CH₂Cl₂/CDCl₃): δ = 29.5.

(vi) **[TiCl₄{Ph₂As(CH₂)₂AsPh₂}]:** Method as for (i) above, red solid, yield 0.26 g, 86%. C₂₆H₂₄As₂Cl₄Ti (676.03): calcd. C 46.2, H 3.6; found C 46.0, H 3.7. – IR: ν_{Ti–Cl} = 401, 385, 377 cm^{–1}. – UV/Vis (λ_{max} × 10³ cm^{–1}): 20.0, 21.7, 25.0, 32.3. – ¹H NMR (CDCl₃, 300 K): δ = 7.7–7.3 (m, Ph), 3.1 (s, CH₂).

(vii) **[TiCl₄{*o*-C₆H₄(AsMe₂)₂}]:** Method as for (i) above, pale orange solid, yield 0.16 g, 62%. C₁₀H₁₆As₂Cl₄Ti (475.79): calcd. C 25.2, H 3.4; found C 25.4, H 3.5. – IR: ν_{Ti–Cl} = 422, 409, 384 cm^{–1}. – UV/Vis (λ_{max} × 10³ cm^{–1}): 21.9, 29.1, 33.0. – ¹H NMR (CDCl₃, 300 K): δ = 7.6 (m, *o*-C₆H₄), 1.75 (s, Me).

(viii) **[TiCl₄{MeC(CH₂AsMe₂)₃}]:** Method as in (i), orange solid, yield 0.22 g, 86%. C₁₁H₂₇As₃Cl₄Ti (573.81): calcd. C 23.0, H 4.7; found C 23.0, H 4.9. – IR: ν_{Ti–Cl} = 400, 375, 368 cm^{–1}. – UV/Vis (λ_{max} × 10³ cm^{–1}): 21.1, 25.3, 27.2, 34.5. – ¹H NMR (CD₂Cl₂, 300 K): δ = 0.95 (AsMe, free), 1.23 (MeC), 1.58, 1.61 (AsMe, coordinated), 1.74 (CH₂, free), 2.15 (m, CH₂, coordinated).

(ix) **[TiCl₄{*o*-C₆H₄(PMe₂)₂}]₂:** Method as in (i), using two molar equivalents of *o*-C₆H₄(PMe₂)₂, golden yellow solid, yield 0.22 g, 85%. C₂₀H₃₂Cl₄P₄Ti (586.08): calcd. C 41.0, H 5.5; found C 40.6, H 5.3. – IR: ν_{Ti–Cl} = 314, 302 sh cm^{–1}. – UV/Vis (λ_{max} × 10³ cm^{–1}): 20.8, 22.5, 24.0, 28.0. – ¹H NMR (CD₂Cl₂, 300 K): δ = 7.5–7.7 (m, *o*-C₆H₄), 1.88 (Me); (183 K): 7.7 (br, *o*-C₆H₄), 1.92 (m, Me). – ³¹P{¹H} NMR (CH₂Cl₂/CDCl₃): δ = 31.5.

(x) **[TiCl₄{*o*-C₆H₄(AsMe₂)₂}]₂:** Method as in (i), using two molar equivalents of *o*-C₆H₄(AsMe₂)₂, bright orange solid, yield 0.30 g,

89%. C₂₀H₃₂As₄Cl₄Ti (761.87): calcd. C 31.5, H 4.2; found C 31.4, H 4.0. – IR: ν_{Ti–Cl} = 323 sh, 317 cm^{–1}. – UV/Vis (λ_{max} × 10³ cm^{–1}): 21.6, 27.6. – ¹H NMR (CD₂Cl₂, 300 K): δ = 7.6 (m, *o*-C₆H₄), 1.8, 1.74, 1.2 (s, Me).

(xi) **[TiBr₄{Ph₂P(CH₂)₃PPh₂}]:** TiBr₄ (0.15 g, 0.41 mmol) was dissolved in refluxing, dry, degassed CH₂Cl₂ (≈30 cm³) in a Schlenk flask under an atmosphere of N₂. After cooling to room temperature, Ph₂P(CH₂)₃PPh₂ (0.17 g, 0.41 mmol) in CH₂Cl₂ (5 cm³), was added to the stirring solution with a syringe, resulting in a dark red solution. The solution was stirred for ca. 30 min., and then the solvent volume was reduced in vacuo to ca. 5 cm³. Dry, degassed hexane (20 cm³) was added to afford a red/orange solid. This solid was filtered, washed with hexane and dried in vacuo. Yield 0.23 g, 73%. C₂₇H₂₆Br₄P₂Ti (779.97): calcd. C 41.5, H 3.3; found C 42.0, H 3.5. – IR: ν_{Ti–Br} = 313, 298, 293 cm^{–1}. – UV/Vis (λ_{max} × 10³ cm^{–1}): 22.5, 32.7. – ¹H NMR (CDCl₃, 300 K): δ = 7.2–8.3 (m, Ph), 3.0–3.6 (br, CH₂). – ³¹P{¹H} NMR (CH₂Cl₂/CD₂Cl₂): δ = 3.5 (broad).

(xii) **[TiBr₄{Ph₂P(CH₂)₂PPh₂}]:** Method as for (xi) above, red solid, yield 0.26 g, 65%. – IR: ν_{Ti–Br} = 309, 299, 292 cm^{–1}. – UV/Vis (λ_{max} × 10³ cm^{–1}): 20.6, 25.5, 34.5. – ¹H NMR (CDCl₃, 300 K): δ = 6.8–7.9 (m, Ph), 4.4–4.8 (m, CH₂). – ³¹P{¹H} NMR (CH₂Cl₂/CDCl₃, 300 K): δ = 13.0 (s); (200 K): δ = 15.4.

(xiii) **[TiBr₄{*o*-C₆H₄(PPh₂)₂}]:** Method as for (xi) above, red/orange solid, yield 0.26 g, 72%. C₃₀H₂₄Br₄P₂Ti (813.98): calcd. C 44.2, H 2.9; found C 44.6, H 3.0. – IR: ν_{Ti–Br} = 315, 310, 304, 301 cm^{–1}. – UV/Vis (λ_{max} × 10³ cm^{–1}): 20.5. – ¹H NMR (CDCl₃, 300 K): δ = 7.0–8.3 (m, Ph, *o*-C₆H₄). – ³¹P{¹H} NMR (CH₂Cl₂/CD₂Cl₂): δ = –10.3 (broad).

(xiv) **[TiBr₄{*o*-C₆H₄(PMe₂)₂}]:** Method as for (xi) above, orange/brown solid, yield 0.16 g, 55%. C₁₀H₁₆Br₄P₂Ti (565.70): calcd. C 21.2, H 2.8; found C 21.6, H 2.9. – IR: ν_{Ti–Br} = 325 sh, 321 cm^{–1}. – UV/Vis (λ_{max} × 10³ cm^{–1}): 21.0, 23.3, 27.7. – ¹H NMR (CD₂Cl₂, 300 K): δ = 7.6 (m, *o*-C₆H₄), 2.03 (m, Me). – ³¹P{¹H} NMR (CH₂Cl₂/CD₂Cl₂): δ = 24.5.

(xv) **[TiBr₄{Ph₂As(CH₂)₂AsPh₂}]:** Method as for (xi) above, red solid, yield 0.33 g, 78%. C₂₆H₂₄As₂Br₄Ti (853.83): calcd. C 36.6, H 2.8; found C 36.3, H 3.0. – IR: ν_{Ti–Br} = 304, 295, 291, 285 cm^{–1}. – UV/Vis (λ_{max} × 10³ cm^{–1}): 18.9, 22.2, 28.6, 32.3. – ¹H NMR (CD₂Cl₂, 300 K): δ = 7.7–7.4 (m, Ph), 3.1 (s, CH₂).

(xvi) **[TiBr₄{*o*-C₆H₄(AsMe₂)₂}]:** Method as for (xi) above, bright red solid, yield 0.17 g, 53%. C₁₀H₁₆As₂Br₄Ti (653.60): calcd. C 18.4, H 2.5; found C 18.4, H 2.5. – IR: ν_{Ti–Br} = 327, 323 cm^{–1}. – UV/Vis (λ_{max} × 10³ cm^{–1}): 20.0, 22.6, 27.2. – ¹H NMR (CD₂Cl₂, 300 K): δ = 7.6 (m, *o*-C₆H₄), 1.9 (s, Me), 1.2 (s, Me).

(xvii) **[TiBr₄{MeC(CH₂AsMe₂)₃}]:** Method as in (xi), red solid, yield 0.27 g, 72%. C₁₁H₂₇As₃Br₄Ti (751.62): calcd. C 17.6, H 3.6; found C 18.1, H 3.7. – IR: ν_{Ti–Br} = 326, 313, 284 cm^{–1}. – UV/Vis (λ_{max} × 10³ cm^{–1}): 19.7, 21.5, 26.7, 32.3. – ¹H NMR (CD₂Cl₂, 300 K): δ = 0.96 (AsMe, free), 1.26 (MeC), 1.71 (br, AsMe, coordinated), 1.75 (CH₂, free), 2.2 (m, CH₂, coordinated).

(xviii) **[TiBr₄{*o*-C₆H₄(PMe₂)₂}]₂:** Method as in (xi), using two molar equivalents of *o*-C₆H₄(PMe₂)₂, bright orange solid, yield 0.16 g, 55%. C₂₀H₃₂Br₄P₄Ti (763.88): calcd. C 31.4, H 4.2; found C 31.2, H 4.0. – IR: ν_{Ti–Br} = 280 br cm^{–1}. – UV/Vis (λ_{max} × 10³ cm^{–1}): 18.9, 21.5, 25.8, 29.0. – ¹H NMR (CD₂Cl₂, 300 K): δ = 7.6–7.8 (m, *o*-C₆H₄), 2.02 (m, Me); (–90 °C): 7.6–7.9 (m, Ph), 2.04–2.00 (m, Me), 1.32 (m, Me). – ³¹P{¹H} NMR (CH₂Cl₂/

Table 1. Crystallographic data

Complex	[TiCl ₄ { <i>o</i> -C ₆ H ₄ -(PMe ₂) ₂ }]	[TiCl ₄ { <i>o</i> -C ₆ H ₄ -(PMe ₂) ₂ }]	[TiBr ₄ { <i>o</i> -C ₆ H ₄ -(PMe ₂) ₂ }]	[TiBr ₄ { <i>o</i> -C ₆ H ₄ -(AsMe ₂) ₂ }]	[TiBr ₄ {MeC(CH ₂ -AsMe ₂) ₃ }]	[TiCl ₅ (Ph ₂ PCH ₂ -PPh ₂)]
Formula	C ₁₀ H ₁₆ Cl ₄ P ₂ Ti	C ₂₀ H ₃₂ Cl ₄ P ₄ Ti	C ₂₀ H ₃₂ Br ₄ P ₄ Ti	C ₂₀ H ₃₂ As ₄ Br ₄ Ti	C ₁₁ H ₂₇ As ₃ Br ₄ Ti	C ₂₅ H ₂₃ Cl ₅ P ₂ Ti
M	387.90	586.08	763.88	939.68	751.62	610.57
Crystal System	orthorhombic	tetragonal	tetragonal	tetragonal	orthorhombic	orthorhombic
Space Group	<i>Pbca</i>	<i>I</i> $\bar{4}$	<i>I</i> $\bar{4}$	<i>I</i> $\bar{4}$	<i>Pna</i> ₂₁	<i>P</i> ₂ ₁ ₂ ₁
<i>a</i> (Å)	13.1752(2)	9.0716(7)	9.1729(4)	9.3125(5)	23.4808(5)	10.4063(6)
<i>b</i> (Å)	15.3631(2)	9.0716(7)	9.1729(4)	9.3125(5)	9.4899(2)	15.3834(9)
<i>c</i> (Å)	16.6348(3)	16.104(1)	16.2896(8)	16.4876(9)	9.9052(2)	16.5893(11)
<i>U</i> (Å ³)	3367.08(8)	1325.2(2)	1370.64(9)	1429.85(12)	2207.18(7)	2655.2(2)
<i>Z</i>	8	2	2	2	4	4
$\mu(\text{Mo-K}\alpha)$ (cm ⁻¹)	13.10	9.75	64.02	105.08	121.05	9.59
Unique obs. reflections	3860	790	722	753	3509	5781
Obs. reflections with [<i>I</i> _o > 3 σ (<i>I</i> _o)]	2461	630	586	633	1769	8136
No. of parameters	154	66	66	66	171	298
<i>R</i> ^[a]	0.037	0.083	0.044	0.048	0.047	0.060
<i>R</i> _w ^[b]	0.047	0.111	0.053	0.053	0.051	0.082

$$^{[a]} R = \Sigma(|F_{\text{obs}}| - |F_{\text{calc}}|)/\Sigma|F_{\text{obs}}|, \quad ^{[b]} R_w = \sqrt{[\Sigma w_i(|F_{\text{obs}}| - |F_{\text{calc}}|)^2]/\Sigma w_i|F_{\text{obs}}|^2}.$$

CDCl₃): δ = 22.2 ([TiBr₄{*o*-C₆H₄(PMe₂)₂}]), 24.3 ([TiBr₄{*o*-C₆H₄(PMe₂)₂}]) and -55 [*o*-C₆H₄(PMe₂)₂].

(xix) [TiBr₄{*o*-C₆H₄(AsMe₂)₂}]: Method as in (xi), using two molar equivalents of *o*-C₆H₄(AsMe₂)₂, red/purple solid, yield 0.36 g, 76%. C₂₀H₃₂As₄Cl₄Ti (761.87): calcd. C 25.6, H 3.4; found C 25.2, H 3.5. - IR: $\nu_{\text{Ti-Br}}$ = 305, 301 cm⁻¹. - UV/Vis (λ_{max} \times 10³ cm⁻¹): 18.5, 20.3, 22.7. - ¹H NMR (CD₂Cl₂, 300 K): see text.

X-ray Crystallography: Details of the crystallographic data collection and refinement parameters are given in Table 1. Crystals of [TiCl₄{*o*-C₆H₄(PMe₂)₂}], [TiCl₄{*o*-C₆H₄(PMe₂)₂}], [TiBr₄{*o*-C₆H₄(PMe₂)₂}], [TiBr₄{*o*-C₆H₄(AsMe₂)₂}] and [TiBr₄{MeC(CH₂AsMe₂)₃}] were obtained by slow evaporation from a solution of the appropriate complex in CH₂Cl₂. The crystals of [TiCl₅(Ph₂PCH₂PPh₂)] were obtained as a hydrolysis product from [TiCl₄(Ph₂PCH₂PPh₂)] in CH₂Cl₂. Data collection was performed with an Enraf-Nonius Kappa CCD diffractometer operating at 150 K, with graphite monochromated Mo-K α radiation (λ = 0.71073 Å). Structure solution and refinement were routine.^[21–24] Crystallographic data (excluding structure factors) for the structure(s) included in this paper have been deposited with the Cambridge Crystallographic Data Centre as supplementary publication no. CCDC-162704–162709. -162704: [TiCl₄{*o*-C₆H₄(PMe₂)₂}], -162705: [TiCl₄{*o*-C₆H₄(PMe₂)₂}], -162706: [TiBr₄{*o*-C₆H₄(PMe₂)₂}], -162707: [TiBr₄{*o*-C₆H₄(AsMe₂)₂}], -162708: [TiBr₄{MeC(CH₂AsMe₂)₃}], -162709: [TiCl₅(Ph₂PCH₂PPh₂)]. Copies of the data can be obtained free of charge on application to CCDC, 12 Union Road, Cambridge CB2 1EZ, UK [Fax: (internat.) + 44-1223/336-033; E-mail: deposit@ccdc.cam.ac.uk].

Acknowledgments

We thank the EPSRC for support and Professor M. B. Hursthouse for access to the Nonius Kappa CCD diffractometer.

^[1] B. Patel, W. Levason, G. Reid, V.-A. Tolhurst and M. Webster, *J. Chem. Soc., Dalton Trans.* **2000**, 3001–3006.

^[2] B. Patel, W. Levason, G. Reid, unpublished work.

^[3] R. J. H. Clark, J. Lewis, R. S. Nyholm, *J. Chem. Soc.* **1962**, 2460–2465.

^[4] R. J. H. Clark, J. Lewis, R. S. Nyholm, P. Pauling, G. B. Robertson, *Nature* **1961**, 192, 222–223.

^[5] R. J. H. Clark, R. H. U. Negrotti, R. S. Nyholm, *J. Chem. Soc., Chem. Commun.* **1966**, 486–487.

^[6] F. A. Cotton, J. H. Matonic, C. A. Murillo, M. A. Petrukhina, *Inorg. Chim. Acta* **1998**, 267, 173–176.

^[7] D. Kepert, K. R. Trigwell, *Aust. J. Chem.* **1975**, 28, 1245–1248.

^[8] W. P. Crisp, R. L. Deutscher, D. L. Kepert, *J. Chem. Soc.* **1970**, 2199–2201.

^[9] R. A. Cipriano, W. Levason, R. A. S. Mould, D. Pletcher, M. Webster, *J. Chem. Soc., Dalton Trans.* **1990**, 339–347.

^[10] R. J. H. Clark, M. L. Greenfield, R. S. Nyholm, *J. Chem. Soc. A* **1966**, 1254–1259.

^[11] A. J. McAlees, R. McCrindle, A. R. Woon-Fat, *Inorg. Chem.* **1976**, 15, 1065–1074.

^[12] F. A. Cotton, C. A. Murillo, M. A. Petrukhina, *J. Organomet. Chem.* **1999**, 573, 78–86.

^[13] F. A. Cotton, C. A. Murillo, M. A. Petrukhina, *J. Organomet. Chem.* **2000**, 593–594, 1–6.

^[14] C. Mahadevan, M. Seshasayee, B. L. Ramakrishna, P. T. Manoharan, *Acta Crystallogr., Sect. C* **1985**, 41, 38–40.

^[15] P. K. Bernstein, G. A. Rodley, R. Marsh, H. B. Gray, *Inorg. Chem.* **1972**, 11, 3040–3043.

^[16] L. F. Warren, M. A. Bennett, *Inorg. Chem.* **1976**, 15, 3126–3140.

^[17] A. Tzschach, W. Lange, *Chem. Ber.* **1962**, 95, 1360–1366.

^[18] R. D. Feltham, R. S. Nyholm, A. Kasenally, *J. Organomet. Chem.* **1967**, 7, 285–288.

^[19] E. P. Kyba, S.-T. Lui, R. L. Harris, *Organometallics* **1983**, 2, 1877–1879.

^[20] H. C. E. McFarlane, W. McFarlane, *Polyhedron* **1983**, 2, 303–304.

^[21] PATTY, The DIRDIF Program System, P. T. Beurskens, G. Admiraal, G. Beurskens, W. P. Bosman, S. Garcia-Granda, R. O. Gould, J. M. M. Smits, C. Smykalla. Technical Report of the Crystallography Laboratory, University of Nijmegen, The Netherlands, **1992**.

^[22] teXsan: Crystal Structure Analysis Package, Molecular Structure Corporation, Texas, **1995**.

^[23] H. D. Flack, *Acta Crystallogr., Sect. A* **1983**, 39, 876–881.

^[24] R. H. Blessing, *Acta Crystallogr., Sect. A* **1995**, 51, 33–38.

Received May 17, 2001

[I01176]